



Published in final edited form as:

Oncogene. 2018 March ; 37(13): 1699–1713. doi:10.1038/s41388-017-0074-2.

Hic-5 Regulates Fibrillar Adhesion Formation to Control Tumor Extracellular Matrix Remodeling through Interaction with Tensin1

Gregory J. Goreczny¹, Ian J. Forsythe¹, and Christopher E. Turner^{1,*}

¹Department of Cell & Developmental Biology, State University of New York Upstate Medical University, Syracuse NY, USA

Abstract

The linearization of the stromal extracellular matrix (ECM) by cancer associated fibroblasts (CAFs) facilitates tumor cell growth and metastasis. However, the mechanism by which the ECM is remodeled is not fully understood. Hic-5 (TGF β 1i1), a focal adhesion scaffold protein, has previously been reported to be crucial for stromal ECM deposition and remodeling *in vivo*. Herein we show that CAFs lacking Hic-5 exhibit a significant reduction in the ability to form fibrillar adhesions, a specialized form of focal adhesion that promote fibronectin fibrillogenesis. Hic-5 was found to promote fibrillar adhesion formation through a newly characterized interaction with tensin1. Furthermore, Src dependent phosphorylation of Hic-5 facilitated the interaction with tensin1 to prevent β 1 integrin internalization and trafficking to the lysosome. The interaction between Hic-5 and tensin1 was mechanosensitive, promoting fibrillar adhesion formation and fibronectin fibrillogenesis in a rigidity dependent fashion. Importantly, this Src dependent mechanism was conserved in three-dimensional (3D) ECM environments. Immunohistochemistry of tensin1 showed enrichment in CAFs *in vivo*, which was abrogated upon deletion of Hic-5. Interestingly, elevated Hic-5 expression correlates with reduced distant metastasis free survival in patients with basal-like, HER2+ and grade 3 tumors. Thus, we have identified Hic-5 as a crucial regulator of ECM remodeling in CAFs by promoting fibrillar adhesion formation through a novel interaction with tensin1.

Keywords

TGF β 1i1; Tumor microenvironment; Mechanosignaling; Breast cancer; Tumor stroma

Users may view, print, copy, and download text and data-mine the content in such documents, for the purposes of academic research, subject always to the full Conditions of use: http://www.nature.com/authors/editorial_policies/license.html#terms

*Correspondence to Dr. Christopher E. Turner, Department of Cell & Developmental Biology, SUNY Upstate Medical University, 750 East Adams Street, Syracuse NY, 13210 USA, Telephone: 315-464-8598, Fax: 315-464-8535, turnerce@upstate.edu.

Conflict of Interest: The authors declare no conflicts of interests

Supplementary Information accompanies the paper on the *Oncogene* website (<http://www.nature.com/onc>).

Introduction

Mammographic dense breast tissue correlates with increased risk of developing cancer and worse patient outcomes(1). Increased tissue rigidity from extracellular matrix (ECM) accumulation in the stroma causes enhanced tumor cell growth and the linearization of collagen fibers at the tumor/stroma boundary is a key step in promoting tumor cell invasion and metastasis(2). Non-transformed fibroblasts actively convert mechanical signals from the ECM into biochemical signals in order to exert an opposing contractile force on the ECM through a process termed tensional homeostasis(3). However, alterations in this mechanism cause a hyperactive mechanical feedback loop, which promote fibroblasts to differentiate into cancer associated fibroblasts (CAF) resulting in enhanced contractility, ECM deposition and linearization to promote a favorable invasive microenvironment for the tumor cells(4). Targeting this ability of the CAFs to deposit and remodel the stromal ECM may provide novel therapies for treating breast cancer.

Mechanical signaling is mediated through focal adhesions, a collection of scaffold and signaling proteins that accumulate via interaction with integrins to provide a physical link between the actin cytoskeleton and the ECM to regulate cell signaling, actin dynamics and gene expression(5). Fibroblasts can generate specialized adhesions, termed fibrillar adhesions, when plated onto fibronectin-rich environments that are characterized as being tensin1-rich, phosphotyrosine poor and by the presence of the $\alpha 5\beta 1$ integrin heterodimer(6). During fibrillar adhesion formation, $\alpha 5\beta 1$ integrins translocate centripetally from stationary $\alpha v\beta 3$ integrin-rich focal adhesions(7). Furthermore $\alpha 5\beta 1$ integrins engage with fibronectin and induces conformational changes to generate a fibrillar matrix in an actomyosin dependent manner(8).

Hic-5 (TGF β 1i1) is a paxillin family member that functions as a molecular scaffold to coordinate numerous molecular interactions and regulate Rho GTPase signaling(9, 10). Furthermore, tyrosine phosphorylation of Hic-5 by FAK and Src family kinases provides additional docking sites for the phosphotyrosine binding SH2 domains of other signaling components(11, 12). We have previously reported that the loss of Hic-5 in CAFs, in the well-established polyoma middle T-antigen (PyMT) breast tumor mouse model, results in their impaired ability to efficiently deposit and remodel the stromal ECM(13). Nevertheless, the mechanism by which Hic-5 regulates ECM remodeling in this context is yet to be determined.

Herein, we have identified Hic-5 as a crucial regulator of fibrillar adhesion formation through a newly characterized interaction with tensin1. Furthermore, Src dependent phosphorylation of Hic-5 was found to be required to promote the interaction with tensin1. Importantly, we found this phosphorylation-dependent mechanism to be conserved in 3D ECM environments and the loss of Hic-5 in the PyMT breast tumor model results in the reduced enrichment of tensin1 in CAFs, *in vivo*. Interestingly, *in-silico* analysis revealed that Hic-5 expression in human breast tumors is highly correlated with a stromal gene expression module and reduced patient survival in a tumor subtype specific pattern. This novel interaction between Hic-5 and tensin1 may represent a key signaling mechanism required for stromal ECM remodeling *in vivo* during human breast tumor progression.

Results

Hic-5 is required for fibrillar adhesion formation

The well-characterized PyMT mouse model undergoes similar stages of tumor progression as the human disease, with a high incidence of metastasis to the lung(14). These characteristics make this model a useful tool to understand human disease progression. We have previously reported a role for Hic-5 in CAFs to promote ECM deposition and remodeling, *in vivo*(13). CAFs derived from the Hic-5 $-/-$ PyMT tumors were not able to efficiently assemble a fibronectin matrix in 2D and 3D environments(13). To understand the mechanism that Hic-5 regulates fibronectin fibril assembly, we initially assessed the distribution of fibrillar adhesions. Fibrillar adhesions are characterized as being rich in tensin1 and have relatively low phosphotyrosine (pY) levels. Accordingly, tensin1 localized to fibrillar adhesions in the Hic-5 $+/-$ CAFs (Figure 1A, arrow). Furthermore, the Hic-5 $-/-$ CAFs exhibited a profound loss of central tensin1-rich, pY-poor fibrillar adhesions (Figure 1A,B). However, tensin1 was still able to localize to peripheral focal adhesions in the Hic-5 $-/-$ CAFs (Figure 1A, inset). Furthermore, transient knockdown of Hic-5 in Human Foreskin Fibroblasts (HFF) showed a similar reduction in the amount of fibrillar adhesions (Supplementary Figure 1), suggesting that Hic-5 plays a key role in fibrillar adhesions formation in other cell types. Western blotting of the Hic-5 $-/-$ CAFs showed a significant reduction in tensin1 protein expression (Figure 1C,D). However, tensin1 mRNA levels were not significantly changed in the Hic-5 $-/-$ CAFs (Figure 1E). The localization and expression of other FA proteins including talin and ILK were not significantly affected by the absence of Hic-5 (Supplementary Figure 2). Importantly, overexpression of GFP-Hic-5 wild-type (WT) in the Hic-5 $-/-$ CAFs partially rescued the ability of these cells to form fibrillar adhesions (Figure 1F,G). Furthermore, the tensin1 MFI is also increased in Hic-5 $-/-$ CAFs overexpressing GFP-Hic-5 WT, suggesting that tensin1 levels can be partially rescued upon reintroduction of Hic-5 (Figure 1H). Together, these data identify a novel and conserved role for Hic-5 in regulating fibrillar adhesion formation in both normal fibroblasts and CAFs.

Hic-5 interacts with tensin1 to promote fibrillar adhesion maturation

Tensin1 is crucial for $\alpha 5\beta 1$ integrin translocation from focal adhesions to form fibrillar adhesions (7). Hic-5 is also required for fibrillar adhesion formation (Figure 1A) and given that Hic-5 and tensin1 colocalize in fibrillar adhesions (Figure 1F), we hypothesized that Hic-5 and tensin1 may directly interact which was subsequently tested using an *in situ* proximity ligation assay (PLA). Distinct clusters of PLA spots were observed in the Hic-5 $+/-$ CAFs at the ends of stress fibers, indicative of an association with focal adhesions (Figure 2A, inset 1). Furthermore, PLA spots were also observed towards the center of the cell, consistent with fibrillar adhesion localization in these cells (Figure 2A, inset 2). Importantly, only background levels of PLA spots were observed between Hic-5 and tensin1 antibodies in the Hic-5 $-/-$ CAFs comparable to an isotype antibody control (Figure 2A,B). Additionally, endogenous Hic-5 and tensin1 were both co-immunoprecipitated in the Hic-5 $+/-$ CAFs (Figure 2C,D), figure demonstrating an association between these two proteins.

The *Hic-5*^{-/-} CAFs exhibited a significant reduction in tensin1 expression (Figure 1C). To determine if tensin1 is sufficient to form fibrillar adhesions in the absence of *Hic-5*, tdTomato-tensin1 was overexpressed in the *Hic-5*^{+/-} and *Hic-5*^{-/-} CAFs (Figure 2E). Quantification of the area of fibrillar adhesions revealed no significant change in the both *Hic-5*^{+/-} CAFs and *Hic-5*^{-/-} CAFs following overexpression of tdTomato-tensin1 (Figure 2F), suggesting that tensin1 is not sufficient to rescue FB in the absence of *Hic-5*. Furthermore, to assess if *Hic-5* is sufficient to generate fibrillar adhesions in the absence of tensin1, RNAi-mediated knockdown of tensin1 was performed (Figure 2G,H). Importantly, *Hic-5* expression was not affected when tensin1 is knocked down (Figure 2G). Using β 1 integrin as a marker of fibrillar adhesions, the tensin1 RNAi-treated CAFs had a significant reduction in the amount of fibrillar adhesions (Figure 2I,J), consistent with previous studies (15, 16). Taken together, these data support a role for *Hic-5* in mediating fibrillar adhesion formation in CAFs through a direct interaction with tensin1.

Hic-5 and tensin1 interact through a phosphorylation dependent mechanism

Src phosphorylation of the β 1 integrin cytoplasmic tail NPxY motif promotes talin dissociation to favor the interaction with tensin1 to form fibrillar adhesions(17, 18). Tensin1 contains an SH2 domain that interacts with proteins that are tyrosine phosphorylated (19). Src also phosphorylates *Hic-5*, providing a potential mechanism to recruit tensin1 to form fibrillar adhesions(11). Treatment of the *Hic-5*^{+/-} CAFs with the Src inhibitor, PP2 caused a dramatic reduction in the amount of fibrillar adhesions (Figure 3A,B). Importantly, PLA between *Hic-5* and phosphotyrosine (pY) antibodies revealed phosphorylated *Hic-5* at the ends of stress fibers and towards the center of the cell (Figure 3C). Conversely, treatment of the *Hic-5*^{+/-} CAFs with the Src inhibitor resulted in a loss PLA spots between *Hic-5* and pY antibodies as compared to vehicle treated cells (Figure 3C,D), indicating that *Hic-5* is phosphorylated in a Src kinase-dependent manner. To determine whether the *Hic-5*-tensin1 interaction is also Src phosphorylation dependent, PLA was performed between *Hic-5* and tensin1 on *Hic-5*^{+/-} CAFs treated with vehicle or PP2 (Figure 3E). Robust PLA spots were clustered at the ends of actin stress fibers in vehicle-treated CAFs (Figure 3E). However, treatment of *Hic-5*^{+/-} CAFs with the Src inhibitor resulted in a dramatic loss of PLA spots between *Hic-5* and tensin1, as compared to vehicle treated cells (Figure 3E,F), demonstrating that the interaction between *Hic-5* and tensin1 is Src-kinase dependent.

To determine whether tensin1 binds preferentially to phosphorylated *Hic-5*, PLA analysis was performed on *Hic-5*^{-/-} CAFs re-expressing GFP-*Hic-5* WT or the non-phosphorylatable GFP-*Hic-5* Y38/60F mutant(11). Interestingly, there was a significant reduction in the number of PLA spots between *Hic-5* Y38/60F and tensin1, suggesting that tensin1 interaction with *Hic-5* requires Y38 and/or Y60 phosphorylation (Figure 3G,H). Furthermore, overexpression of GFP-*Hic-5* Y38/60F in the *Hic-5*^{-/-} CAFs was not able to rescue fibrillar adhesion formation, as compared to GFP-*Hic-5* WT overexpressing cells (Figure 3I,J), suggesting that *Hic-5* phosphorylation is required for this process.

Hic-5 is required for Beta 1 integrin stability on the cell surface

Tensin1 directly interacts with the actin cytoskeleton and the β 1 integrin tail, which stabilizes β 1 integrin on the cell surface(20, 21). Given this stabilizing role for tensin1, we

assessed the distribution of $\beta 1$ integrin. Using an antibody that recognizes the active form of $\beta 1$ integrin (9EG7), Hic-5 +/- CAFs showed robust staining in central, tensin1-containing fibrillar adhesions and peripheral focal adhesions (Figure 4A). However, analysis of the Hic-5 -/- CAFs showed that while active $\beta 1$ integrin is still able to localize to peripheral focal adhesions, the majority of its distribution was cytoplasmic (Figure 4A,B). Time-lapse imaging of Hic-5 +/- and Hic-5 -/- CAFs was performed to assess whether the focal adhesions were disassembling at a faster rate which could account for the increased cytoplasmic $\beta 1$ integrin distribution (Figure 4C, Supplemental Movies 1 and 2). Quantification of the disassembly rate and lifetime of peripheral and central associated adhesions in the Hic-5 +/- CAFs showed that the peripheral adhesions disassembled faster than central adhesions albeit the overall lifetime was not significantly different (Figure 4D,E). Similar measurements in the Hic-5 -/- CAFs revealed that both peripheral and centrally-associated adhesions disassembled twice as fast (Figure 4D) and the overall lifetime of the adhesions in the Hic-5 -/- CAFs was significantly reduced (Figure 4E), suggesting that integrin complexes are being internalized at a faster rate.

$\beta 1$ integrin is internalized and trafficked through endosomal compartments to be recycled back to the cell surface or sent to the lysosome for degradation(22). Western blotting showed a significant reduction in total $\beta 1$ integrin expression in the Hic-5 -/- CAFs lysates (Figure 4F,G). Furthermore, there was a distinct reduction of the mature, 125 kDa band of $\beta 1$ integrin in these cells suggesting that the protein was being turned over rapidly(23). Indeed, the cytoplasmic distribution of $\beta 1$ integrin in the Hic-5 -/- CAFs was found to be localized preferentially with LAMP-1 positive lysosomes (Figure 4H,I). Additionally, treatment of the Hic-5 -/- CAFs with the lysosomal inhibitor, chloroquine, significantly increased the ratio of mature to immature $\beta 1$ integrin in the Hic-5 -/- CAFs (Figure 4J,K). Therefore, Hic-5 expression suppresses $\beta 1$ integrin internalization and degradation to facilitate the formation of fibrillar adhesions.

The Hic-5-tensin1 interaction is mechanosensitive

Biomechanical signals from the ECM are transduced through integrin complexes to sense and respond to the changes in ECM composition and rigidity(4). Interestingly, previous reports have shown that both Hic-5 and tensin1 are mechanosensors(24–26). To determine whether substrate rigidity influenced the Hic-5 and tensin1 interaction, PLA was performed on Hic-5 +/- CAFs plated onto glass (hard) and a soft (~1kPa) PDMS substrate (Figure 5A). Quantification of the number of PLA spots revealed a significant reduction between Hic-5 and tensin1 in cells plated on soft substrates (Figure 5B). Importantly, there is no significant difference in the cell area of the Hic-5 +/- CAFs plated onto hard and soft substrates ($9732\mu\text{m}^2 \pm 1481\mu\text{m}^2$ to $8093\mu\text{m}^2 \pm 465\mu\text{m}^2$, $p=0.35$). We also observed a significant reduction in the amount of fibrillar adhesions when Hic-5 +/- CAFs are plated on soft substrates (Figure 5C,D), showing that fibrillar adhesion formation requires increased substrate rigidity. Furthermore, the Hic-5 -/- CAFs were not able to sense the changes in rigidity to generate fibrillar adhesions as compared to the control CAFs (Figure 5C,D). The ability of the Hic-5 +/- CAFs to assemble fibronectin into fibers on the cell surface was also significantly reduced when they were plated on soft PDMS (Figure 5E,F). However, Hic-5 -/- CAFs were unable to efficiently assemble fibronectin fibers on either hard or soft

substrates, consistent with their inability to generate fibrillar adhesions (Figure 5E,F). Taken together, the Hic-5 and tensin1 interaction is driven by increased substrate rigidity to promote fibrillar adhesion formation and fibronectin fibrillogenesis.

Src dependent Hic-5 and tensin1 interaction is conserved in 3D environments

The mechanosensory and matrix remodeling capabilities, *in vivo*, requires the formation of 3D matrix adhesions(27). These structures are reminiscent of 2D fibrillar adhesions as they have been characterized as long, thin structures (up to 19 μm long), rich in $\alpha 5\beta 1$ along with robust tensin1 localization(28). To assess if Hic-5 promotes 3D matrix adhesions formation similar to 2D fibrillar adhesion formation, Hic-5 +/- and Hic-5 -/- CAFs were plated into Human Fibroblast (HFF)-generated 3D cell derived matrices (3D CDMs). Hic-5 +/- CAFs exhibited characteristic tensin1-rich elongated 3D matrix adhesions (Figure 6A). However, adhesions in the Hic-5 -/- CAFs were significantly shorter and had reduced tensin1 localization (Figure 6A,B). Interestingly, we also observed a lack of centrally located 3D matrix adhesions in the Hic-5 -/- CAFs, suggesting a similar mechanism of central adhesion formation as in 2D. PLA was performed to assess whether Src phosphorylation of Hic-5 was required for tensin1 interaction in 3D ECM environments. Indeed, we observed robust PLA spots between Hic-5 and tensin1 clustered at the ends of actin stress fibers in vehicle-treated cells (Figure 6C). Quantification of the number of PLA spots revealed that the number of PLA spots was significantly reduced in Hic-5 +/- CAFs treated with the Src inhibitor (Figure 6C,D).

Hic-5 promotes breast tumor growth, invasion and metastasis through the deposition and remodeling of the stromal ECM(13). Given that tensin1 and Hic-5 interact in 3D environments, we wanted to assess the tensin1 distribution in the Hic-5 -/- PyMT tumors. Immunohistochemistry (IHC) revealed that tensin1 was highly enriched in the CAFs in the Hic-5 +/- PyMT tumor but not the tumor cells (Figure 6E, arrow), similar to the distribution of Hic-5, *in vivo*(13). Strikingly, tensin1 was not enriched in the CAFs in the Hic-5 -/- PyMT tumor sections, but tensin1 expression was observed in nearby blood vessels (Figure 6E), suggesting that the loss of tensin1 may contribute to the reduced ECM remodeling observed in the Hic-5 -/- PyMT mouse. Additionally, immunohistochemical analysis of human breast tumors revealed Hic-5 and tensin1 co-localization in α -Smooth Muscle Actin positive CAFs (Figure 6F), suggesting that the Hic-5-dependent ECM remodeling mechanism described herein may also play a role during human breast tumor progression

Hic-5 expression correlates to poor patient prognosis

To further evaluate a potential connection between Hic-5 expression and outcome of human breast cancer patients, Kaplan-Meier survival analysis was performed using the publicly available GOBO online tool(29). Although Hic-5 expression in breast tumors did not correlate with poor outcome when all tumor types were examined together (Figure 7A), discriminating between distinct tumor subtypes using the PAM50 classifier revealed that patients with high Hic-5 expression correlated with reduced Distant Metastasis Free Survival (DMFS) in both HER2+ (Figure 7B) and Basal-like tumors (Figure 7C), while there was no significant correlation in luminal A and luminal B tumors (Supplemental Figure 3A,B). Additionally, delineating between tumor grades revealed no correlation to reduced DMFS in

grade 1 and 2 tumors, but high Hic-5 expression in grade 3 tumors was associated with reduced DMFS (Figure 7D, Supplemental Figure 3C,D). Interestingly, Hic-5 expression in the breast tumors analyzed also correlated highly with a stroma-associated gene module (Figure 7E, $p < 1 \times 10^{-10}$, Supplemental Figure 3E). Lastly, while the aforementioned correlations were derived from total tumor data, a limited microarray analysis of isolated CAFs from distinct tumor subtypes showed that both Hic-5 and tensin1 expression was specifically enriched in HER2+ tumors (30). Collectively, these data suggest that Hic-5 plays a prominent role in the stroma of human breast cancer patients and further analysis is warranted.

Discussion

The ability of CAFs to remodel the ECM of the stroma around the primary tumor provides physical tracks that tumor cells utilize to invade and metastasize(31). Thus, understanding the molecular mechanism that drives stromal matrix remodeling will be important for the design of targeted therapies to alleviate tumor growth and invasion. Herein, we report a previously unappreciated interaction between the focal adhesion proteins Hic-5 and tensin1, that is required to generate fibrillar adhesions to promote ECM remodeling (Figure 1A, 2A).

Fibrillar adhesions are a specialized form of cell-ECM adhesion that translocate centripetally from peripheral focal adhesions to facilitate the formation of fibronectin fibrils. We have shown that Hic-5 is a novel component of fibrillar adhesions and its localization is necessary for the formation of these structures (Figure 1A,F). Previous studies have shown the importance of Integrin Linked Kinase (ILK) in regulating fibrillar adhesion formation through recruiting tensin1 to focal adhesions(32). Importantly, the lack of Hic-5 does not alter expression or localization of ILK to focal adhesions (Supp. Figure 2B,C) and ectopically expressing tensin1 in the Hic-5 $-/-$ CAFs cannot rescue fibrillar adhesion formation (Figure 2E,F). These data suggest that Hic-5 is a key mediator of fibrillar adhesion formation and ILK and tensin1 are not sufficient to promote their formation. Furthermore, despite paxillin, a close relative of Hic-5, being expressed in the Hic-5 $-/-$ CAFs and its ability to interact with ILK(33), it is not sufficient to promote fibrillar adhesions(13). As fibrillar adhesions assemble, paxillin has been shown to be dephosphorylated(34) in contrast to Hic-5 phosphorylation, which we showed, is required for fibrillar adhesion formation (Figure 3I,J) revealing another distinct and opposing function of these two proteins(35).

Although tensin1 can localize to focal adhesions in the absence of Hic-5 (Figure 1A), Src phosphorylation of Hic-5 drives the interaction between tensin1 and Hic-5 to promote fibrillar adhesion formation (Figure 3E,F). Tensin1 contains an SH2 domain that interacts with tyrosine-phosphorylated proteins(19). Interestingly, the binding specificity of the tensin1 SH2 domain is regulated by p38MAPK(36). Serine/threonine phosphorylation of tensin1 promotes its dissociation from the RhoGAP, Deleted in cancer-1 (DLC1), to promote interactions with pY proteins including p130CAS(37). In our study, we determined that tensin1 also interacts with tyrosine phosphorylated Hic-5 (Figure 3G,H), potentially through the tensin1 SH2 domain. Hic-5 has been shown to regulate p38MAPK activity in a TGF β -induced invadopodia model(11). Furthermore, the loss of p38MAPK in a heart injury mouse

model resulted in a reduced fibrotic response(38). This raises the intriguing possibility that Hic-5 may coordinate its interaction with tensin1 by regulating the specificity of the tensin1 SH2 domain through a p38MAPK-dependent feedback loop.

Talin dissociates from the Src phosphorylated NPxY motif of $\beta 1$ integrin to promote the “switch” to tensin1 to facilitate fibrillar adhesion formation(17). We have shown that Hic-5 plays a central role in recruiting tensin1 to form fibrillar adhesions and to prevent $\beta 1$ integrin internalization and degradation (Figures 2,4). Clathrin adaptors Dab2 and Numb contain a phosphotyrosine-binding (PTB) domain similar to tensin1, which bind to the NPxY-motif of $\beta 1$ integrin to promote clathrin-dependent internalization(39, 40). Furthermore, the recruitment of the AP-2 clathrin adaptor complex to focal adhesions is mediated through an interaction between actopaxin (α -parvin), a Hic-5 binding partner, and $\beta 2$ -adapatin(41, 42). It is conceivable that during fibrillar adhesion formation, Hic-5 mediates the interaction between tensin1 and the $\beta 1$ integrin NPxY-motif to prevent association with clathrin adaptor proteins to inhibit internalization. Furthermore, $\beta 1$ integrin is trafficked preferentially to the lysosome in the Hic-5 $-/-$ CAFs (Figure 4H), suggesting that Hic-5 may play a role in regulating $\beta 1$ integrin recycling to the cell surface. Further analysis will have to be performed to assess how Hic-5 may regulate integrin trafficking.

Downstream signaling from $\alpha 5\beta 1$ integrin engagement with the ECM regulates force generation through RhoA/Rock dependent myosin II activity(43). Rigidity dependent myosin II-generated forces are required to promote a tensioned fibronectin/ $\alpha 5\beta 1$ integrin catch bond to generate fibronectin fibrils(44, 45). Hic-5 may be crucial to strengthen the fibronectin/integrin bond in a rigidity dependent manner by recruiting tensin1 and thus associating $\beta 1$ integrin with the actin cytoskeleton (Figure 5A,B). Consistent with this notion, recent work has shown that tensin1 and tensin3 are required to maintain $\beta 1$ integrin in an activated state during fibrillar adhesion formation(15). Furthermore, the Hic-5 $-/-$ CAFs are inherently less contractile suggesting that they cannot exert sufficient force to promote high affinity integrin linkages to fibronectin and thus resulting in the internalization of $\beta 1$ integrin (Figure 4A)(13). Interestingly, the deposition and organization of the collagen matrix *in vivo* is also dependent on fibronectin fibrillogenesis(46). Fibrillar collagen constitutes the major component of the tumor ECM and contributes to the rigidity and tensile strength of the tissue(47). The inability of the Hic-5 $-/-$ CAFs to assemble a robust FN matrix in 2D and 3D environments may be a cause for reduced collagen deposition observed in the Hic-5 $-/-$ PyMT tumors(13). Thus, it will be important to further evaluate how Hic-5 regulates the deposition and composition of the ECM in this setting.

The existence of aligned collagen fibers, oriented perpendicular to the tumor boundary, promotes tumor cell invasion and correlates with an overall reduced patient survival(48). We have shown, using the PyMT breast tumor mouse model, that the linearization of the ECM is a Hic-5-dependent process(13). Survival analysis of human patients revealed that high Hic-5 expression in patients with HER2+ and basal-like breast cancer correlated with reduced distant metastasis free survival. Interestingly, HER2+ and basal-like tumors are significantly more rigid, indicative of enhanced ECM deposition, as compared to luminal A and B tumors and are generally considered to be more aggressive(49). Importantly however, the potential contribution of Hic-5 expression in the primary tumor cells, where it may function in their

EMT and invasion cannot be overlooked when evaluating these datasets(50, 51). Nevertheless, the subtype specific correlation of Hic-5 expression warrants further characterization and analysis in additional human patient samples and is critical to understand the role of Hic-5 in CAF activity, *in vivo*. Furthermore, future studies aimed at designing drugs that specifically target the tumor microenvironment to be used either alone or in combination with conventional therapies may provide more effective options to treat the disease.

Material and Methods

Cancer Associated Fibroblast (CAF) isolation and cell culture

The Hic-5 +/- PyMT and Hic-5 -/- PyMT CAFs were isolated and maintained as previously described(13). Human Foreskin Fibroblasts (HFF) were maintained in CDM media (DMEM supplemented with 10% FBS, 2mM L-glutamate, 10 I.U. penicillin/10µg/mL streptomycin, and 1mM Sodium pyruvate) at 37°C with 5% CO₂. All cell lines were routinely stained with DAPI to assess potential mycoplasma contamination.

Antibodies and reagents

Antibodies used in this analysis were: Hic-5 611164, β1 integrin clone 9EG7 553715, CD29 610467, ILK 611803 (BD Biosciences, Franklin Lakes, NJ USA); tensin1 NBP1-84129 (Novus Biologicals, Littleton, CO, USA); phosphotyrosine clone 4G10 05-321 (Millipore); talin T3287, fibronectin F3648, α-tubulin clone DM1A T9026, α-actinin A5044, tensin1 SAB200283 (Sigma-Aldrich, St. Louis, MO, USA); phosphotyrosine clone P-Tyr-100 9411 (Cell Signaling, Danvers, MA, USA); β1 integrin clone 12G10 ab30394 (Abcam, Cambridge, MA, USA); LAMP1 bs-1970R (Bioss, Woburn, MA, USA); Epcam G8.8 was deposited to the DSHB by Farr, A.G.

F-actin was visualized using Rhodamine phalloidin (Thermo-Fisher, Carlsbad, CA, USA) or Actistain 670 (Cytoskeleton, Denver, CO, USA). Fluorescently conjugated secondary antibodies used were: Dylight 488, 550 and 633 conjugated anti-mouse and anti-rabbit were purchased from Thermo-Fisher. FITC anti-rat, Alexa-fluor 488 anti-mouse, HRP-conjugated anti-mouse and anti-rabbit secondary antibodies were purchased from Jackson ImmunoResearch. The polydimethylsiloxane (PDMS) substrates were prepared as previously described(52).

SiRNA and plasmid transfections

Tensin1 RNAi-mediated knockdown was performed using 10µM siRNA and Lipofectamine RNAiMAX (Life Technologies, Carlsbad, CA). The siRNA were ON-TARGETplus mouse tensin1 (L-040925, SMARTpool) and control (D-001810, Non-Targeting Pool) purchased from Dharmacon (Lafayette, CO, USA). Hic-5 RNAi-mediated knockdown was performed using 40µM siRNA and Oligofectamine. The siRNA oligonucleotides were purchased from Ambion and the siRNA sequences have been described previously(11).

For overexpression studies, Hic-5 +/- or Hic-5 -/- CAFs were transfected with GFP, GFP-Hic-5 WT, or GFP-Hic-5 Y38/60F using Lipofectamine 3000 (Invitrogen). The Hic-5 constructs were generated as described previously(11).

Immunofluorescence and Immunohistochemistry

Immunofluorescence and immunohistochemical staining of cell and tumor sections was performed as described previously(13). Fresh frozen, OCT embedded human tumor sections were obtained from the tumor bank at the University of Massachusetts Medical School (Worcester, MA, USA).

Fibrillar adhesions were quantified as the ratio of the central, tensin1-rich, pY-poor, elongated adhesion area relative to the total cell area using the threshold function of ImageJ. Similarly, fibronectin fibrillogenesis was quantified by thresholding fibronectin fibers relative to the cell area.

Cell derived matrix generation

Three-dimensional cell-derived matrices (CDMs) were generated as previously described(13).

Analysis of focal adhesion dynamics

Adhesion dynamics were quantified as previously described(50). Briefly, Hic-5 +/- and Hic-5 -/- CAFs were infected with GFP-talin Baculovirus (Thermo-Fisher) with the BacMAM enhancer 24 hours prior to imaging. The cells were re-plated onto 10µg/mL fibronectin for 4 hours before imaging using a Nikon TE2000 microscope equipped with an environmental chamber, a perfect focus automated multipoint visiting stage and imaged using a HCX Plan Fluotar 10x/0.30 NA objective with images taken every 2 minutes for 3 hours.

Proximity ligation assay

Proximity ligation assay (PLA) was performed using the anti-Mouse MINUS probe, anti-Rabbit PLUS probe and the orange detection reagent (Sigma-Aldrich) as previously described(53). Actin was visualized using actistain 670 and imaged on a Leica scanning confocal (SP5) with a HCX Plan Apochromat 63x/1.40-0.60 NA oil λ blue objective. The total number of distinct PLA spots per cell were quantified using the threshold function of ImageJ.

Quantitative Polymerase Chain Reaction

The primers used were mouse tensin1 (Forward 5'-GTTTCTCCAAGCATAACAGCCA-3' and Reverse 5'-GTTTCAGAGAGGTTGAATAGCAGG-3') and mouse GAPDH (Forward 5'-GTGTTCCCTACCCCAATGTGT-3' and Reverse 5'-ATTGTCATACCAGGAAATGAGCTT-3'). The PCR was run on a BioRad CRX384 Touch Real-Time PCR detection system using BioRad iQ SYBR Green Supermix (170-8880) with the following conditions: 95°C for 2 minutes followed by 40 cycles: 95°C, 5 seconds and 58°C, 30 seconds followed by 95°C for 5 seconds. The melt curves were obtained from

65°C to 95°C and Tensin1 mRNA levels were normalized to GAPDH using the Cq method.

Coimmunoprecipitation and Western blotting

Cells were lysed in 50mM Tris-HCL pH 7.6, 1% Triton X-100, 150mM NaCl, 10% glycerol, 10µg/mL aprotinin, 10µg/mL leupeptin, and 1mM PMSF. Lysates were cleared at 10,000×g for 10 minutes and incubated with the appropriate primary antibody for 2 hours at 4°C. 20µL of protein A/G beads were added for another 1 hour, washed 3X and resuspended in SDS sample buffer. Western blotting was performed as previously described(11).

Kaplan-Meier Analysis

Kaplan-Meier survival analysis for Hic-5 (TGFB1i1) was evaluated using the gene-expression based-outcome for breast cancer online tool (GOBO, <http://co.bmc.lu.se/gobo/gsa.pl>)(29).

Statistical analysis

Two-tailed Student's t-tests were performed to determine statistical significance using Microsoft Excel. All the data are represented by the mean ± the SEM and performed 3 times unless otherwise indicated. * p<0.05, ** p<0.005, and *** p<0.0005.

Supplementary Material

Refer to Web version on PubMed Central for supplementary material.

Acknowledgments

Financial Support: National Institutes of Health Grant R01 CA163296 and R01 GM047607 to CET and the Carol M Baldwin Breast Cancer Research Fund of CNY awards to CET.

We would like to thank members of the Turner lab for helpful discussions and critical reading of this manuscript and thank Theresa Stowell for performing the qPCR analyses. This work was supported by the National Institutes of Health Grant R01 CA163296, R01 GM047607 and the Carol M Baldwin Breast Cancer Research Fund of CNY awards to CET.

References

1. Boyd NF, Rommens JM, Vogt K, Lee V, Hopper JL, Yaffe MJ, et al. Mammographic breast density as an intermediate phenotype for breast cancer. *Lancet Oncol.* 2005; 6(10):798–808. [PubMed: 16198986]
2. Pickup MW, Mouw JK, Weaver VM. The extracellular matrix modulates the hallmarks of cancer. *EMBO Rep.* 2014; 15(12):1243–53. [PubMed: 25381661]
3. Paszek MJ, Zahir N, Johnson KR, Lakins JN, Rozenberg GI, Gefen A, et al. Tensional homeostasis and the malignant phenotype. *Cancer Cell.* 2005; 8(3):241–54. [PubMed: 16169468]
4. Provenzano PP, Keely PJ. Mechanical signaling through the cytoskeleton regulates cell proliferation by coordinated focal adhesion and Rho GTPase signaling. *J Cell Sci.* 2011; 124(Pt 8):1195–205. [PubMed: 21444750]
5. Schwartz MA. Integrins and extracellular matrix in mechanotransduction. *Cold Spring Harb Perspect Biol.* 2010; 2(12):a005066. [PubMed: 21084386]
6. Zamir E, Katz M, Posen Y, Erez N, Yamada KM, Katz BZ, et al. Dynamics and segregation of cell-matrix adhesions in cultured fibroblasts. *Nat Cell Biol.* 2000; 2(4):191–6. [PubMed: 10783236]

7. Pankov R, Cukierman E, Katz BZ, Matsumoto K, Lin DC, Lin S, et al. Integrin dynamics and matrix assembly: tensin-dependent translocation of alpha(5)beta(1) integrins promotes early fibronectin fibrillogenesis. *J Cell Biol.* 2000; 148(5):1075–90. [PubMed: 10704455]
8. Singh P, Carraher C, Schwarzbauer JE. Assembly of fibronectin extracellular matrix. *Annu Rev Cell Dev Biol.* 2010; 26:397–419. [PubMed: 20690820]
9. Thomas SM, Hagel M, Turner CE. Characterization of a focal adhesion protein, Hic-5, that shares extensive homology with paxillin. *J Cell Sci.* 1999; 112(Pt 2):181–90. [PubMed: 9858471]
10. Brown MC, Turner CE. Paxillin: adapting to change. *Physiol Rev.* 2004; 84(4):1315–39. [PubMed: 15383653]
11. Pignatelli J, Tumbarello DA, Schmidt RP, Turner CE. Hic-5 promotes invadopodia formation and invasion during TGF-beta-induced epithelial-mesenchymal transition. *J Cell Biol.* 2012; 197(3):421–37. [PubMed: 22529104]
12. Fujita H, Kamiguchi K, Cho D, Shibnuma M, Morimoto C, Tachibana K. Interaction of Hic-5, A senescence-related protein, with focal adhesion kinase. *J Biol Chem.* 1998; 273(41):26516–21. [PubMed: 9756887]
13. Goreczny GJ, Ouderkirk-Pecone JL, Olson EC, Krendel M, Turner CE. Hic-5 remodeling of the stromal matrix promotes breast tumor progression. *Oncogene.* 2017; 36(19):2693–703. [PubMed: 27893716]
14. Lin EY, Jones JG, Li P, Zhu L, Whitney KD, Muller WJ, et al. Progression to malignancy in the polyoma middle T oncoprotein mouse breast cancer model provides a reliable model for human diseases. *Am J Pathol.* 2003; 163(5):2113–26. [PubMed: 14578209]
15. Georgiadou M, Lilja J, Jacquemet G, Guzman C, Rafeeva M, Alibert C, et al. AMPK negatively regulates tensin-dependent integrin activity. *J Cell Biol.* 2017; 216(4):1107–21. [PubMed: 28289092]
16. Rainero E, Howe JD, Caswell PT, Jamieson NB, Anderson K, Critchley DR, et al. Ligand-Occupied Integrin Internalization Links Nutrient Signaling to Invasive Migration. *Cell Rep.* 2015
17. Legate KR, Fassler R. Mechanisms that regulate adaptor binding to beta-integrin cytoplasmic tails. *J Cell Sci.* 2009; 122(Pt 2):187–98. [PubMed: 19118211]
18. Volberg T, Romer L, Zamir E, Geiger B. pp60(c-src) and related tyrosine kinases: a role in the assembly and reorganization of matrix adhesions. *J Cell Sci.* 2001; 114(Pt 12):2279–89. [PubMed: 11493667]
19. Davis S, Lu ML, Lo SH, Lin S, Butler JA, Druker BJ, et al. Presence of an SH2 domain in the actin-binding protein tensin. *Science.* 1991; 252(5006):712–5. [PubMed: 1708917]
20. Lo SH, Janmey PA, Hartwig JH, Chen LB. Interactions of tensin with actin and identification of its three distinct actin-binding domains. *J Cell Biol.* 1994; 125(5):1067–75. [PubMed: 8195290]
21. Torgler CN, Narasimha M, Knox AL, Zervas CG, Vernon MC, Brown NH. Tensin stabilizes integrin adhesive contacts in *Drosophila*. *Dev Cell.* 2004; 6(3):357–69. [PubMed: 15030759]
22. Caswell PT, Vadrevu S, Norman JC. Integrins: masters and slaves of endocytic transport. *Nat Rev Mol Cell Biol.* 2009; 10(12):843–53. [PubMed: 19904298]
23. Bottcher RT, Stremmel C, Meves A, Meyer H, Widmaier M, Tseng HY, et al. Sorting nexin 17 prevents lysosomal degradation of beta1 integrins by binding to the beta1-integrin tail. *Nat Cell Biol.* 2012; 14(6):584–92. [PubMed: 22561348]
24. Kim-Kaneyama JR, Suzuki W, Ichikawa K, Ohki T, Kohno Y, Sata M, et al. Uni-axial stretching regulates intracellular localization of Hic-5 expressed in smooth-muscle cells in vivo. *J Cell Sci.* 2005; 118(Pt 5):937–49. [PubMed: 15713747]
25. Deakin NO, Ballestrem C, Turner CE. Paxillin and Hic-5 interaction with vinculin is differentially regulated by Rac1 and RhoA. *PLoS One.* 2012; 7(5):e37990. [PubMed: 22629471]
26. Stutchbury B, Atherton P, Tsang R, Wang DY, Ballestrem C. Distinct focal adhesion protein modules control different aspects of mechanotransduction. *J Cell Sci.* 2017; 130(9):1612–24. [PubMed: 28302906]
27. Doyle AD, Yamada KM. Mechanosensing via cell-matrix adhesions in 3D microenvironments. *Exp Cell Res.* 2016; 343(1):60–6. [PubMed: 26524505]
28. Cukierman E, Pankov R, Stevens DR, Yamada KM. Taking cell-matrix adhesions to the third dimension. *Science.* 2001; 294(5547):1708–12. [PubMed: 11721053]

29. Ringner M, Fredlund E, Hakkinen J, Borg A, Staaf J. GOBO: gene expression-based outcome for breast cancer online. *PLoS One*. 2011; 6(3):e17911. [PubMed: 21445301]
30. Tchou J, Kossenkov AV, Chang L, Satija C, Herlyn M, Showe LC, et al. Human breast cancer associated fibroblasts exhibit subtype specific gene expression profiles. *BMC Med Genomics*. 2012; 5:39. [PubMed: 22954256]
31. Lu P, Weaver VM, Werb Z. The extracellular matrix: a dynamic niche in cancer progression. *J Cell Biol*. 2012; 196(4):395–406. [PubMed: 22351925]
32. Stanchi F, Grashoff C, Nguemeni Yonga CF, Grall D, Fassler R, Van Obberghen-Schilling E. Molecular dissection of the ILK-PINCH-parvin triad reveals a fundamental role for the ILK kinase domain in the late stages of focal-adhesion maturation. *J Cell Sci*. 2009; 122(Pt 11):1800–11. [PubMed: 19435803]
33. Nikolopoulos SN, Turner CE. Integrin-linked kinase (ILK) binding to paxillin LD1 motif regulates ILK localization to focal adhesions. *J Biol Chem*. 2001; 276(26):23499–505. [PubMed: 11304546]
34. Zaidel-Bar R, Milo R, Kam Z, Geiger B. A paxillin tyrosine phosphorylation switch regulates the assembly and form of cell-matrix adhesions. *J Cell Sci*. 2007; 120(Pt 1):137–48. [PubMed: 17164291]
35. Deakin NO, Pignatelli J, Turner CE. Diverse roles for the paxillin family of proteins in cancer. *Genes Cancer*. 2012; 3(5–6):362–70. [PubMed: 23226574]
36. Hall EH, Balsbaugh JL, Rose KL, Shabanowitz J, Hunt DF, Brautigan DL. Comprehensive analysis of phosphorylation sites in Tensin1 reveals regulation by p38MAPK. *Mol Cell Proteomics*. 2010; 9(12):2853–63. [PubMed: 20798394]
37. Zhao Z, Tan SH, Machiyama H, Kawauchi K, Araki K, Hirata H, et al. Association between tensin 1 and p130Cas at focal adhesions links actin inward flux to cell migration. *Biol Open*. 2016; 5(4): 499–506. [PubMed: 27029899]
38. Molkenin JD, Bugg D, Ghearing N, Dorn LE, Kim P, Sargent MA, et al. Fibroblast-Specific Genetic Manipulation of p38 MAPK in vivo Reveals its Central Regulatory Role in Fibrosis. *Circulation*. 2017
39. Chao WT, Kunz J. Focal adhesion disassembly requires clathrin-dependent endocytosis of integrins. *FEBS Lett*. 2009; 583(8):1337–43. [PubMed: 19306879]
40. Ezratty EJ, Bertaux C, Marcantonio EE, Gundersen GG. Clathrin mediates integrin endocytosis for focal adhesion disassembly in migrating cells. *J Cell Biol*. 2009; 187(5):733–47. [PubMed: 19951918]
41. Pignatelli J, Jones MC, LaLonde DP, Turner CE. Beta2-adaptin binds actopaxin and regulates cell spreading, migration and matrix degradation. *PLoS One*. 2012; 7(10):e46228. [PubMed: 23056266]
42. Nikolopoulos SN, Turner CE. Actopaxin, a new focal adhesion protein that binds paxillin LD motifs and actin and regulates cell adhesion. *J Cell Biol*. 2000; 151(7):1435–48. [PubMed: 11134073]
43. Schiller HB, Hermann MR, Polleux J, Vignaud T, Zanivan S, Friedel CC, et al. beta1- and alpha-class integrins cooperate to regulate myosin II during rigidity sensing of fibronectin-based microenvironments. *Nat Cell Biol*. 2013; 15(6):625–36. [PubMed: 23708002]
44. Carraher CL, Schwarzbauer JE. Regulation of matrix assembly through rigidity-dependent fibronectin conformational changes. *J Biol Chem*. 2013; 288(21):14805–14. [PubMed: 23589296]
45. Friedland JC, Lee MH, Boettiger D. Mechanically activated integrin switch controls alpha5beta1 function. *Science*. 2009; 323(5914):642–4. [PubMed: 19179533]
46. Kadler KE, Hill A, Canty-Laird EG. Collagen fibrillogenesis: fibronectin, integrins, and minor collagens as organizers and nucleators. *Curr Opin Cell Biol*. 2008; 20(5):495–501. [PubMed: 18640274]
47. Kolacna L, Bakesova J, Varga F, Kostakova E, Planka L, Necas A, et al. Biochemical and biophysical aspects of collagen nanostructure in the extracellular matrix. *Physiol Res*. 2007; 56(Suppl 1):S51–60. [PubMed: 17552894]
48. Conklin MW, Eickhoff JC, Riching KM, Pehlke CA, Eliceiri KW, Provenzano PP, et al. Aligned collagen is a prognostic signature for survival in human breast carcinoma. *Am J Pathol*. 2011; 178(3):1221–32. [PubMed: 21356373]

49. Acerbi I, Cassereau L, Dean I, Shi Q, Au A, Park C, et al. Human breast cancer invasion and aggression correlates with ECM stiffening and immune cell infiltration. *Integr Biol (Camb)*. 2015; 7(10):1120–34. [PubMed: 25959051]
50. Deakin NO, Turner CE. Distinct roles for paxillin and Hic-5 in regulating breast cancer cell morphology, invasion, and metastasis. *Mol Biol Cell*. 2011; 22(3):327–41. [PubMed: 21148292]
51. Tumbarello DA, Turner CE. Hic-5 contributes to epithelial-mesenchymal transformation through a RhoA/ROCK-dependent pathway. *J Cell Physiol*. 2007; 211(3):736–47. [PubMed: 17299801]
52. Wormer DB, Davis KA, Henderson JH, Turner CE. The focal adhesion-localized CdGAP regulates matrix rigidity sensing and durotaxis. *PLoS One*. 2014; 9(3):e91815. [PubMed: 24632816]
53. Deakin NO, Turner CE. Paxillin inhibits HDAC6 to regulate microtubule acetylation, Golgi structure, and polarized migration. *J Cell Biol*. 2014; 206(3):395–413. [PubMed: 25070956]

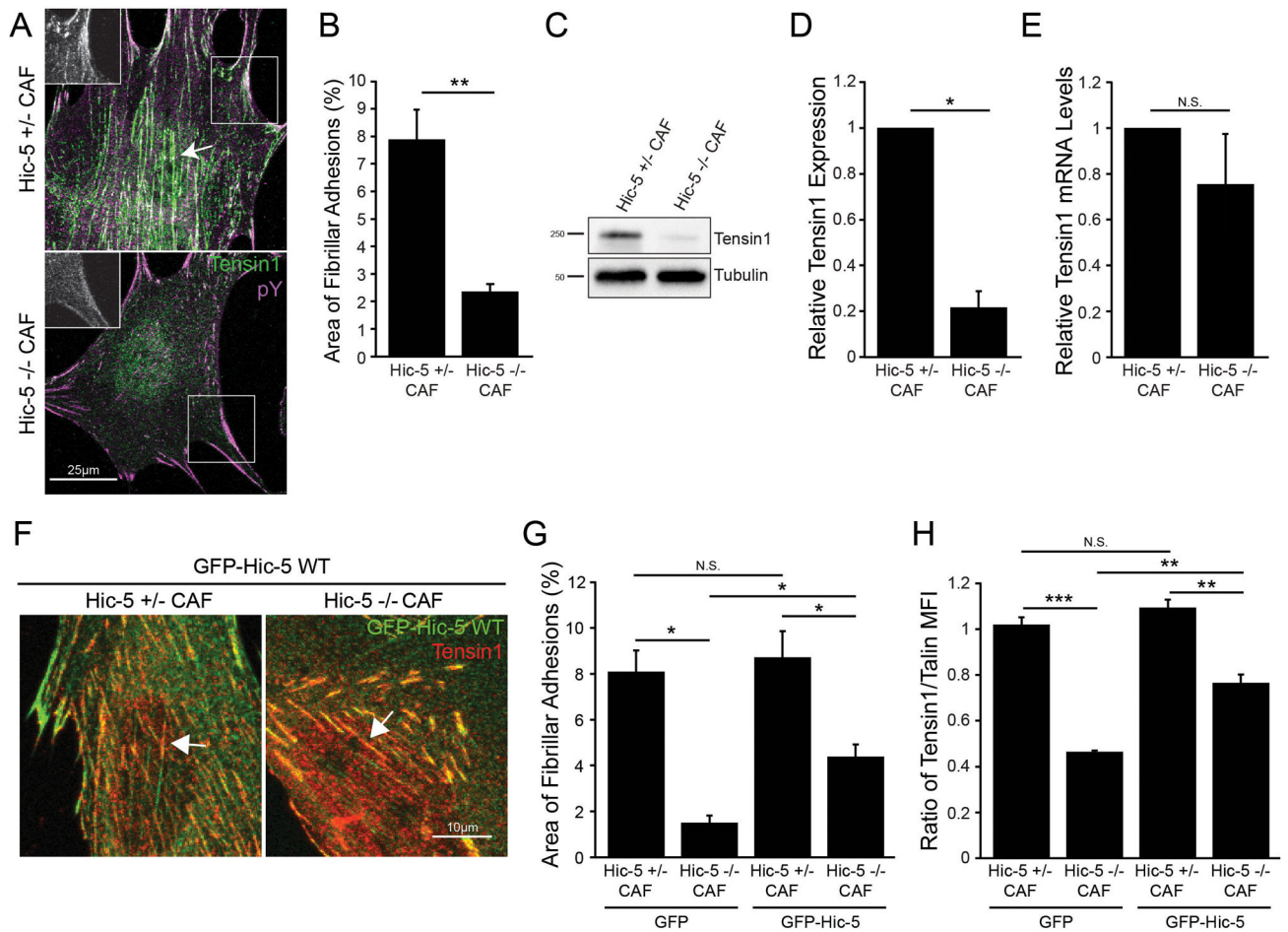


Figure 1. Hic-5 is required for fibrillar adhesion formation

A) Representative images of tensin1 and phosphotyrosine (pY) staining in the Hic-5 +/- and Hic-5 -/- CAFs. The arrow indicates a tensin1-rich, pY-poor fibrillar adhesion. B) Quantification of the area of fibrillar adhesions in the CAFs. n=3 independent experiments. C) Western blotting of tensin1 expression and (D) quantification of the relative tensin1 expression. n=3 independent experiments. E) qPCR analysis of tensin1 mRNA levels in the Hic-5 +/- and Hic-5 -/- CAFs. n=3 independent experiments. F) Representative images of Hic-5 +/- and Hic-5 -/- CAFs overexpressing GFP-Hic-5 WT. The arrow indicates fibrillar adhesions. G) Quantification of the area of fibrillar adhesions. n=3 independent experiments. H) Quantification of the ratio of tensin1 MFI to talin MFI. n=3 independent experiments. The data represent the mean +/- SEM and statistical significance was determined using a Student's T-test. * p<0.05, ** p<0.005, *** p<0.0005.

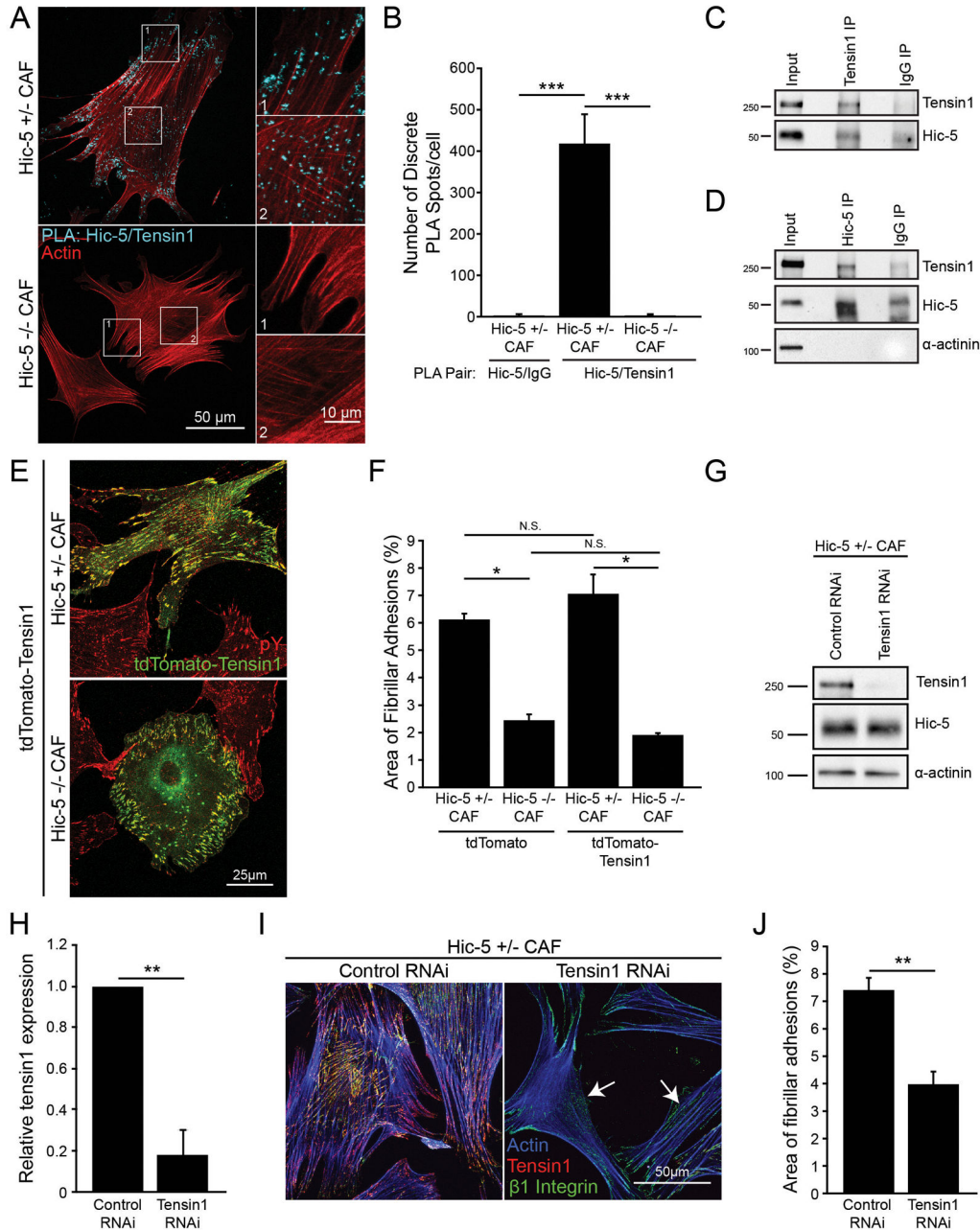


Figure 2. Hic-5 interacts with tensin1 to promote fibrillar adhesion formation

A) Representative Proximity Ligation Assay (PLA) between Hic-5 and tensin1 in Hic-5 +/- and Hic-5 -/- CAFs. Inset 1 indicates PLA spots clustered at the ends of stress fibers. Inset 2 indicates PLA spots in the center of the cell. B) Quantification of the number of distinct PLA spots per cell. n=3 independent experiments. C) Representative co-immunoprecipitation (co-IP) showing Hic-5 is pulled down using a tensin1 antibody. n=2 independent experiments. D) Representative co-IP showing tensin1 is pulled down using a Hic-5 antibody. n=2 independent experiments. E) Representative images of Hic-5 +/- and Hic-5 -/- CAFs overexpressing tdTomato-tensin1. F) Quantification of the area of fibrillar

adhesions per cell. n=3 independent experiments. G) Representative Western blot of Hic-5 +/- CAFs treated with tensin1 RNAi (L-040925, SMARTpool) and (H) quantification of the relative tensin1 protein expression. n=3 independent experiments. I) Representative images of tensin1 RNAi-treated Hic-5 +/- CAFs stained for active B1 integrin (9EG7) and tensin1. The arrows indicate cells with a reduced amount of fibrillar adhesions. J) Quantification of the area of fibrillar adhesions per cell. n=3 independent experiments. The data represent the mean +/- SEM and statistical significance was determined using a Student's T-test. * p<0.05, ** p<0.005, *** p<0.0005.

Author Manuscript

Author Manuscript

Author Manuscript

Author Manuscript

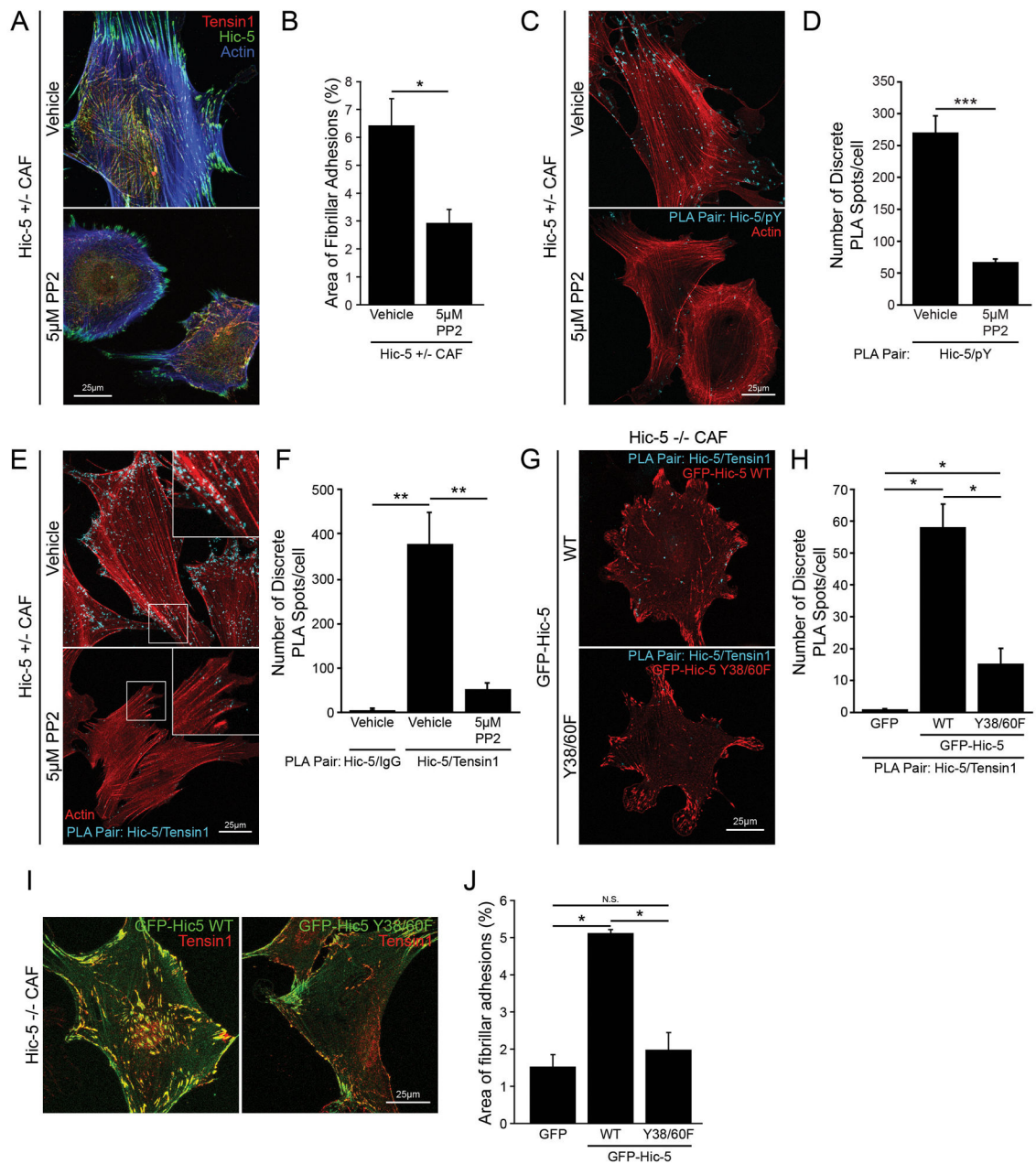


Figure 3. Hic-5 interaction with tensin1 is Src-phosphorylation dependent

A) Representative images of Hic-5 +/- CAFs treated with vehicle or 5µM of the Src-kinase inhibitor, PP2. B) Quantification of the area of fibrillar adhesions per cell. n=3 independent experiments. C) Representative Hic-5 and pY PLA in vehicle or 5µM PP2-treated CAFs and (D) quantification of the number of PLA spots per cell. n=3 independent experiments. E) Representative Hic-5 and tensin1 PLA of Hic-5 +/- CAFs treated with vehicle or 5µM PP2. F) Quantification of the number of distinct PLA spots per cell. n=3 independent experiments. G) Representative PLA between Hic-5 and tensin1 in Hic-5 -/- CAFs overexpressing GFP-Hic-5 WT or GFP-Hic-5 Y38/60F and (H) Quantification of the number of distinct PLA spots. n=3 independent experiments. I) Representative images of

Hic-5 +/- CAFs overexpressing GFP-Hic-5 WT and GFP-Hic-5 Y38/60F and (J)
Quantification of the area of fibrillar adhesions per cell. n=3 independent experiments. The data represent the mean +/- SEM and statistical significance was determined using a Student's T-test. * p<0.05, ** p<0.005, *** p<0.0005.

Author Manuscript

Author Manuscript

Author Manuscript

Author Manuscript

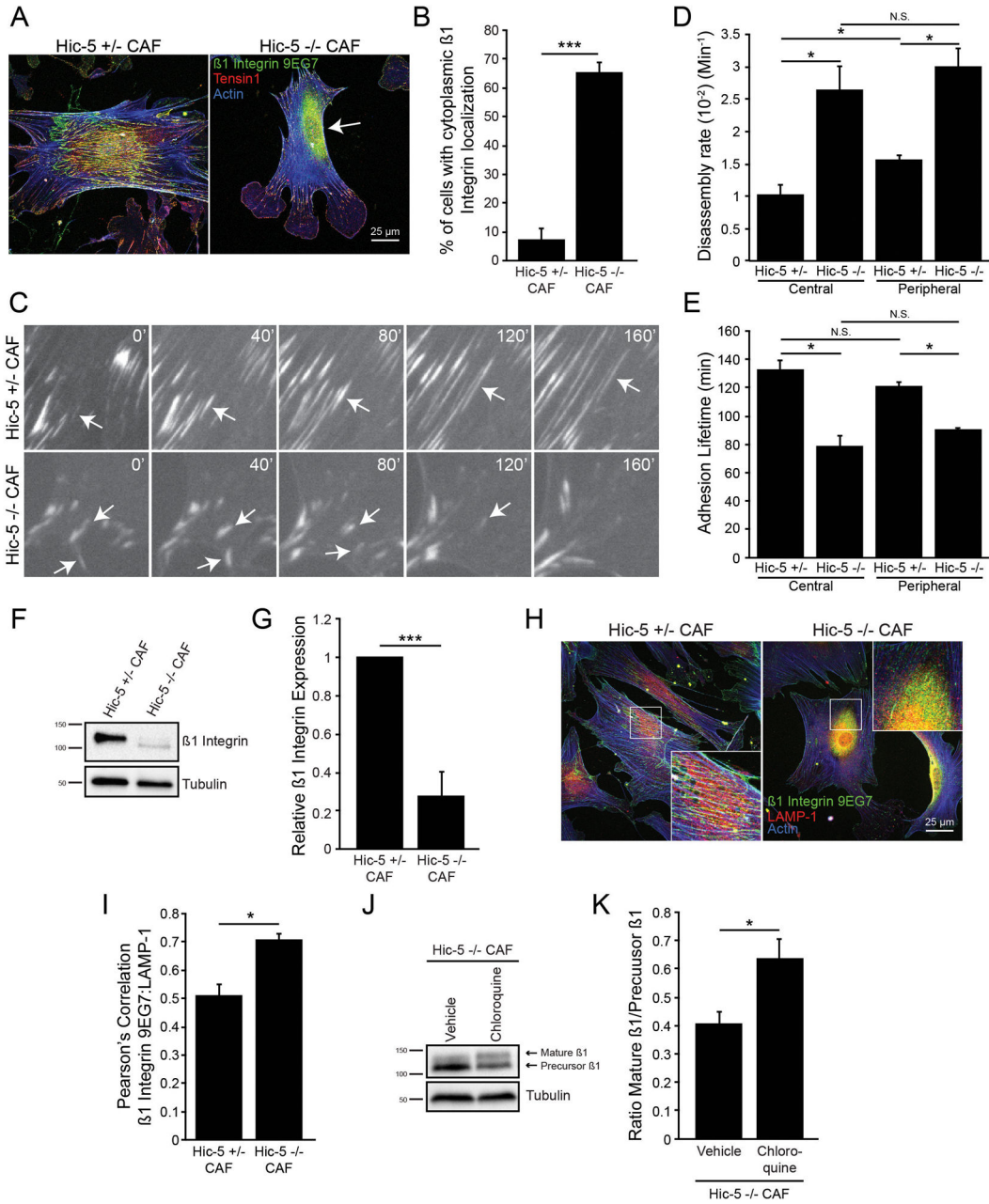


Figure 4. Hic-5 promotes β1 integrin stability on the cell surface

A) Representative images of Hic-5 +/- and Hic-5 -/- CAFs stained for active β1 integrin (9EG7) and tensin1. The arrow indicates cytoplasmic accumulation of β1 integrin. B) Quantification of the percentage of cells that have a cytoplasmic distribution of β1 integrin. n=3 independently performed experiments. C) Representative montages from time-lapse movies of GFP-talin-labeled focal adhesions in the Hic-5 +/- and Hic-5 -/- CAFs. D) Quantification of the disassembly rate and (E) adhesion lifetime of central and peripheral adhesions in GFP-talin infected cells. F) Representative Western blot and (G) quantification of β1 integrin expression in the Hic-5 +/- and Hic-5 -/- CAFs. n=3 independent experiments. H) Representative images of Hic-5 +/- and Hic-5 -/- CAFs stained for β1

integrin and LAMP-1 and (I) Quantification of the Pearson's correlation between $\beta 1$ integrin and LAMP-1. n=3 independent experiments. J) Representative Western blot of Hic-5 $-/-$ CAFs treated with 25 μ M chloroquine and (K) Quantification of the ratio of the mature $\beta 1$ to the precursor $\beta 1$ integrin. n=3 independent experiments. The data represents the mean \pm SEM and statistical significance was determined using a Student's T-test. * $p < 0.05$, *** $p < 0.0005$.

Author Manuscript

Author Manuscript

Author Manuscript

Author Manuscript

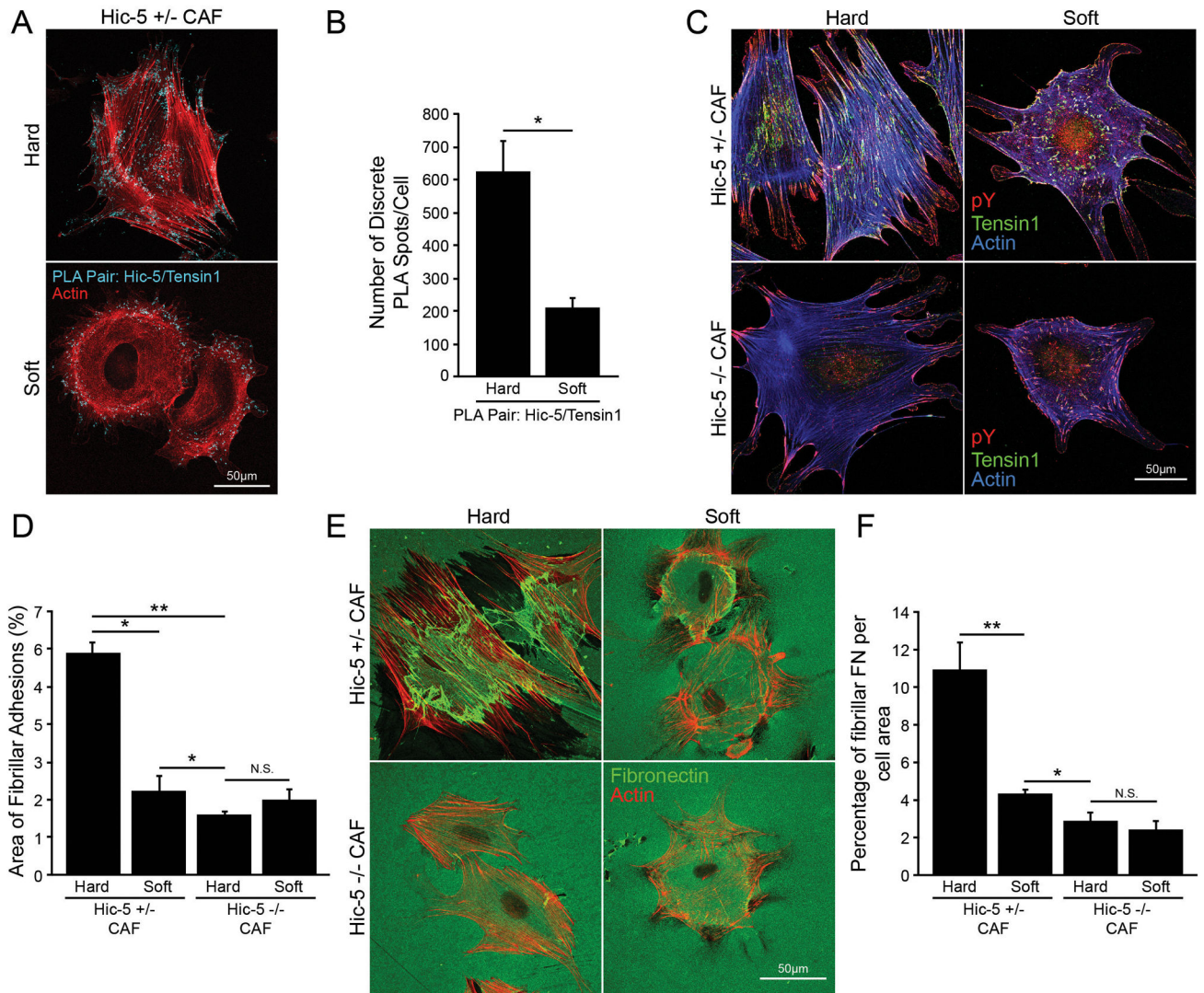


Figure 5. Hic-5 interaction with tensin1 is mechanosensitive

A) Representative PLA of Hic-5 and tensin1 in Hic-5 +/- CAFs plated on glass (hard) or a soft PDMS substrate. B) Quantification of the average number of distinct PLA spots per cell. n=3 independent experiments. C) Representative images of Hic-5 +/- and Hic-5 -/- CAFs plated on glass (hard) and a soft PDMS substrate stained for tensin1 and pY. D) Quantification of the area of fibrillar adhesions per cell, n=3 independent experiments. E) Representative images of fibronectin fibrillogenesis by Hic-5 +/- and Hic-5 -/- CAFs plated on glass (hard) or soft PDMS substrate. F) Quantification of the area of fibronectin fibers per cell. n=3 independent experiments. The data represent the mean +/- SEM and statistical significance was determined using a Student's T-test. * p<0.05, ** p<0.005.

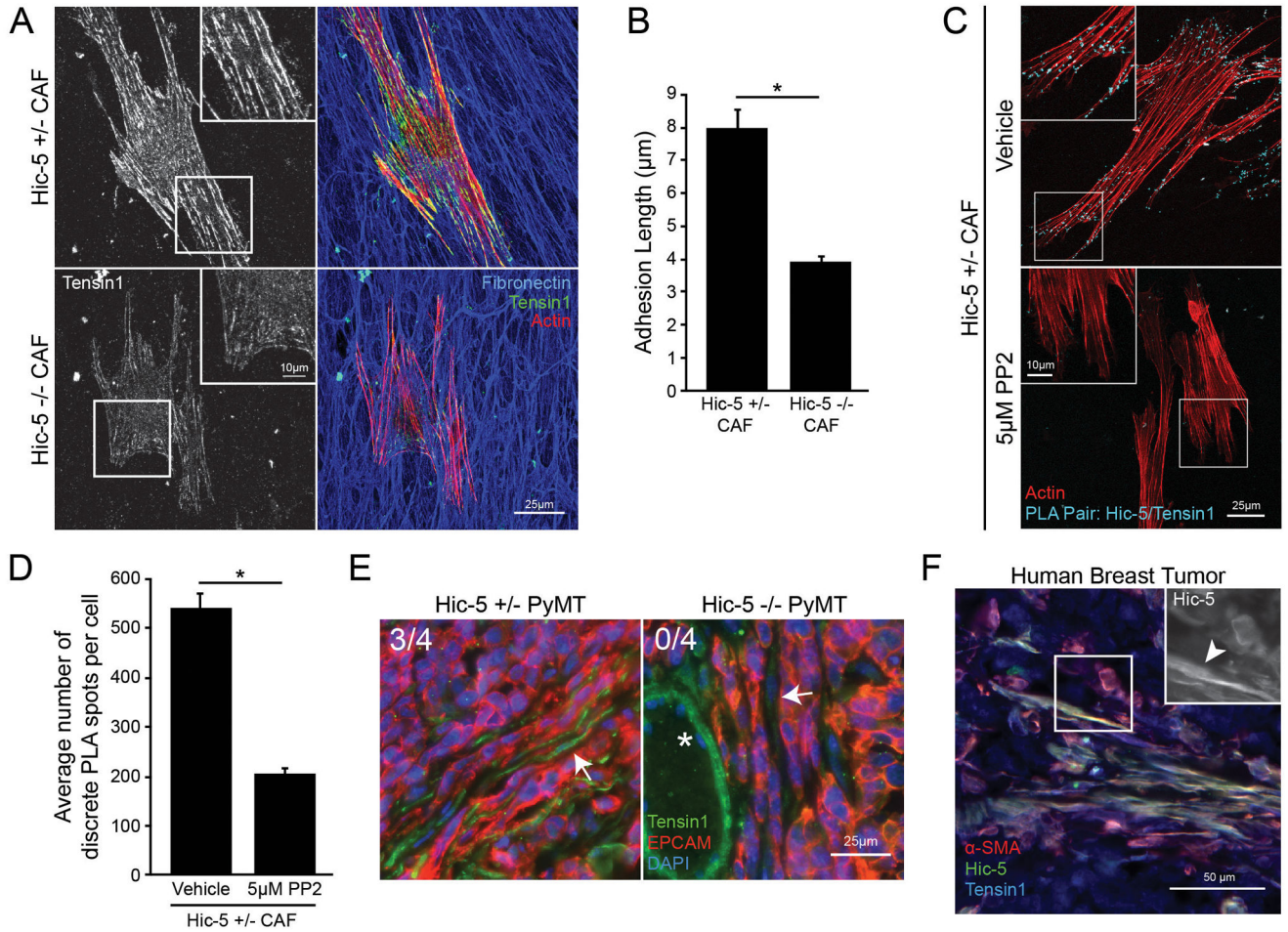


Figure 6. Src dependent Hic-5 and tensin1 interaction is conserved in 3D matrix environments

A) Representative images of tensin1 staining in Hic-5 +/- and Hic-5 -/- CAFs migrating in a human fibroblast (HFF)-derived 3D CDMs. B) Quantification of the average focal adhesion length. n=3 independent experiments. C) Representative images of PLA between Hic-5 and tensin1 in vehicle or 5µM PP2 treated Hic-5 +/- CAFs spread in 3D CDMs. D) Quantification of the number of distinct PLA spots per cell. n=3 independent experiments. E) Representative IHC of tensin1 staining in Hic-5 +/- PyMT and Hic-5 -/- PyMT breast tumor sections. The arrows indicate CAFs in the tumor and the asterisk indicates positive tensin1 expression in a blood vessel. Tensin1 was expressed in CAFs in 3/4 Hic-5 +/- PyMT and 0/4 Hic-5 -/- PyMT tumors. F) Immunohistochemistry of Hic-5, tensin1 and α-SMA staining in a human breast tumor sample. The arrowhead indicates a tensin1 and Hic-5 positive CAF. The data represent the mean +/- SEM and statistical significance was determined using a Student's T-test. * p<0.05.

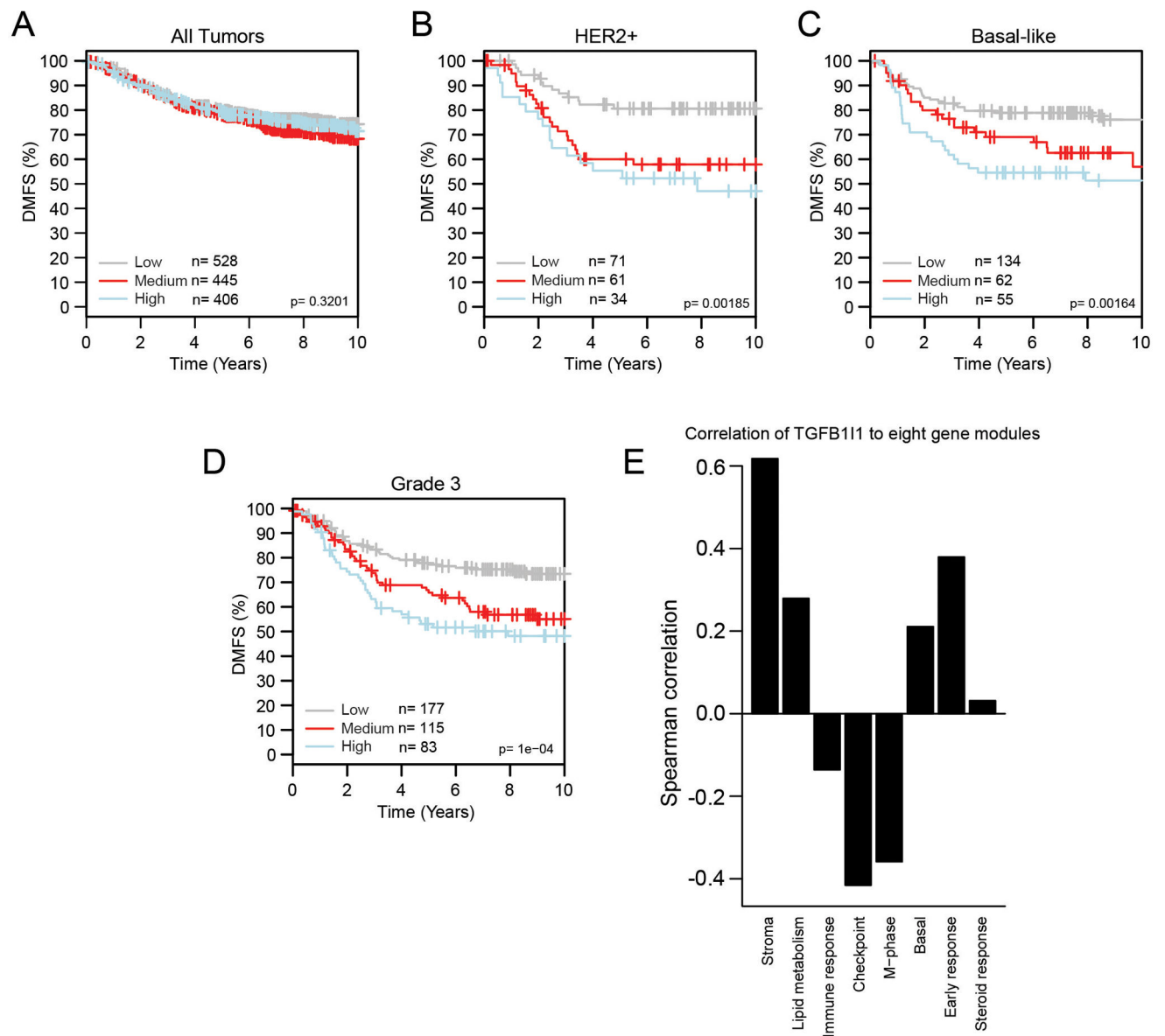


Figure 7. Hic-5 expression in breast tumors correlates with reduced patient survival

A–D) Hic-5 (TGFB111) expression was interrogated using the GOBO online tool to generate Kaplan-Meier Survival curves (29). A) Hic-5 correlation to patient outcome compiled from all tumors, irrespective of tumor subtype and tumor grade. n=1379 patients, B) HER2+ tumors, n=166 patients, C) Basal-like tumors, n=251 patients, and D) Grade 3 tumors, n=375 patients. E) Correlation between Hic-5 expression and eight distinct gene expression modules generated from the GOBO tool, demonstrating a high correlation between Hic-5 expression and stroma-associated genes.